

# Perspective Transformation Layer

Nishan Khatri<sup>1</sup>, Agnibh Dasgupta<sup>1</sup>, Yucong Shen<sup>2</sup>, Xin Zhong<sup>1\*</sup> and Frank Shih<sup>2</sup>

<sup>1</sup>University of Nebraska Omaha

<sup>2</sup>New Jersey Institute of Technology

{nkhatri@unomaha.edu, adasgupta@unomaha.edu, ys496@njit.edu,  
xzhong@unomaha.edu, shih@njit.edu}

## Abstract

Incorporating geometric transformations that reflect the relative position changes between an observer and an object into computer vision and deep learning models has attracted much attention in recent years. However, the existing proposals mainly focus on affine transformations that cannot fully show viewpoint changes. Furthermore, current solutions often apply a neural network module to learn a single transformation matrix, which ignores the possibility for various viewpoints and creates extra to-be-trained module parameters. In this paper, a layer (PT layer) is proposed to learn the perspective transformations that not only model the geometries in affine transformation but also reflect the viewpoint changes. In addition, being able to be directly trained with gradient descent like traditional layers such as convolutional layers, a single proposed PT layer can learn an adjustable number of multiple viewpoints without training extra module parameters. The experiments and evaluations confirm the superiority of the proposed PT layer.

## 1 Introduction

Human vision is often insusceptible to viewpoint changes; for example, we are able to recognize an object regardless of the object's presenting angle. In computer vision, realizing such an insusceptible viewpoint is of great interest because it can provide robustness [Lowe, 2004] to a lot of application scenarios such as the classification and object detection [Xu *et al.*, 2018; Pan *et al.*, 2019]. One efficient approach to respond to the relative position changes between an observer and an object is to perform geometric transformations [Wang *et al.*, 2018; Krasheninnikov and Potapov, 2012], where the geometry of an image is changed by projecting the coordinates without altering the pixel values. Typical linear and efficient geometric transformations include affine transformations that capture the rotation, scaling, translation, and shearing of an object; and perspective transformations (PT) that indicate how the perception of objects change when an observer's viewpoint varies.

\*Contact Author

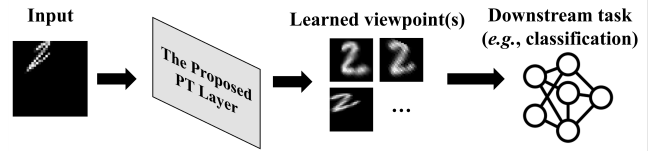


Figure 1: General process of the proposed PT layer.

Although convolutional neural networks (CNNs) have achieved the state-of-the-art performance in many computer vision applications [He *et al.*, 2016; Wang *et al.*, 2019; Huang *et al.*, 2017], due to the fragility of the neural networks under geometric distortions [Papernot *et al.*, 2016; Zhou *et al.*, 2017], appropriately responding to the geometric transformations within deep learning frameworks remains a key challenge. Traditional CNNs try to address this geometric distortion issue through data augmentation and local pooling layers. Although data augmentation that adds geometric distortions into the training dataset could introduce some geometry information to a CNN model, there is no performance guarantee for untrained transformations. Consequently, prior knowledge in a specific problem domain is often required to determine the to-be-augmented operations, which is not always feasible. On the other hand, the local pooling layers (e.g. a  $2 \times 2$  or  $3 \times 3$  local max pooling) can only mitigate the impact of translations after many rounds of downsampling. In addition, translation is just one simple instance of geometric transformation. Hence, local pooling layers are not an applicable solution to model geometric transformations in deep learning.

Modeling geometric transformations in deep learning has attracted increased attention in recent years [Jaderberg *et al.*, 2015; Lin and Lucey, 2017; Detlefsen *et al.*, 2018; Esteves *et al.*, 2018; Tai *et al.*, 2019]. One most representative idea is to learn a transformation matrix (TM) by a CNN module. So, if the CNN module is inserted into a deep learning model and the learned TM is applied to transform some feature maps, a geometric transformation can be simultaneously trained with other layers. However, there still exists challenging issues. For example, in most existing work, the learning outcomes focus on affine transformations that only relate to four operations (*i.e.*, the rotation, scaling, translation, and shearing) while there can be a lot more possible geometries in various applications. Also, one CNN module often outputs a single TM, which only learns one possible transformation. However, it can be beneficial to analyze multiple viewpoints

even just for a single object [Andrew, 2001]. Finally, existing solutions often create extra CNN modules to learn a TM, which introduces extra to-be-trained module parameters that increase the model complexity.

To address the above challenges, in the context of deep learning frameworks, we propose a PT layer that can learn PTs for the downstream tasks (see Figure 1). The merits are threefold: (i) The proposed layer learns PT which not only captures the geometries in affine transformation but also reflects the viewpoint changes; (ii) One proposed PT layer can learn multiple TMs, therefore providing multiple viewpoints for possible analysis; Furthermore, the learning capacity of the PT layer can be tuned due to the adjustability of the TM number; and (iii) The proposal is a layer that directly trains its TMs inside with gradient descent. So, no extra module parameters are needed.

The remainder of this paper is organized as follows. The related work is described in Section 2. Details of the proposed PT layer is presented in Section 3. Experiments and analysis are presented in Section 4. Finally, conclusions are drawn in Section 5.

## 2 Related Work

In this section, we briefly review the related work that incorporates geometric transformations in deep learning. The general process is developing a CNN module that outputs a geometric TM, and jointly training the module with other layers by transforming some feature maps with this TM.

The spatial transformer network (STN) [Jaderberg *et al.*, 2015] was the first effort to model geometric transformations for neural nets. The STN proposed a modular CNN block that can be inserted into some selected positions of a deep learning architecture. An STN module can learn to affine transform its inputs, so that the rotation, scaling, translation, and shearing can be trained together with other layers in an end-to-end manner.

Later, there were many proposed improvements of STN. Incorporating a cascade of STNs to collect the geometric transformations, [Lin and Lucey, 2017] proposed an inverse compositional STN that established a connection between the classical Lucas-Kanade algorithm [Lucas and Kanade, 1981] and the STN, so that the geometric transformations in the data can be mitigated through multiple spatial transformations with alignments. [Detlefsen *et al.*, 2018] proposed a deep diffeomorphic transformer networks that developed a diffeomorphic continuous piecewise affine (CPAB) based transformation, and created two modules that learns affine and CPAB respectively. Combining the ideas of STN and canonical coordinate representations, [Esteves *et al.*, 2018] proposed a polar transformer network that achieved the invariance to translations and equivariance to rotations and dilations. One recent and most successful improvement of STN is the equivariant transformer network (ETN) [Tai *et al.*, 2019] that proposed to sequentially connect a canonical coordinates transformation and a STN module. Compared to STN, ETN improved the robustness to some continuous transformations.

There were also a few proposals involving viewpoints in some specific applications. For example, [Garau *et al.*, 2021]

proposed to apply the capsule network [Sabour *et al.*, 2017] to capture the equivalent viewpoint information for human poses. [Yan *et al.*, 2016] proposed an encoder-decoder network to learn a perspective information for three-dimensional object reconstruction with only two-dimensional supervision.

Thus far, most of the existing methods focus the affine transformation that cannot reflect viewpoint changes. Also, a separate CNN network or module is often required to learn one transformation, which ignores the multi-view analysis and creates extra to-be-trained module parameters. To the best of our knowledge, our proposed PT layer is the first method that can learn multiple PTs (viewpoints) with a single layer, and can directly train its TMs with gradient descent without requiring additional module parameters.

## 3 The Proposed PT Layer

This section discusses the details of our proposed PT layer. Specifically, we talk about PT layer’s overview in Section 3.1, transformation, interpolation in Section 3.2, and back-propagation in Section 3.3.

### 3.1 Overview

Figure 2 conceptually illustrates the proposed PT layer, where the  $\otimes$  denotes an interpolation. As compared to the STN and ETN, one PT layer learns more parameters each TM (*i.e.*, learning the PT instead of the affine), allows a self-definable number of TMs, and directly trains its TMs (while the STN and ETN train a CNN module to output one TM).

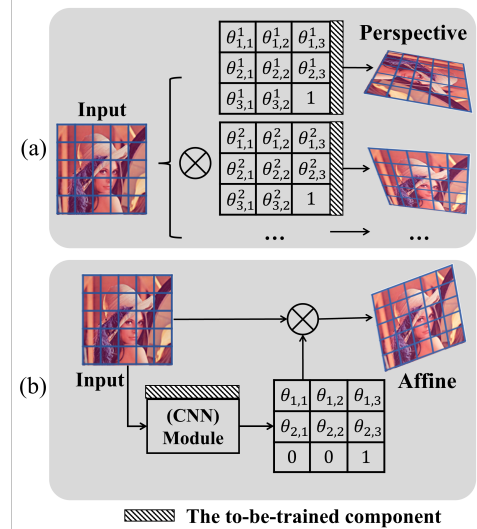


Figure 2: Conceptual illustrations. (a) The proposed PT layer; (b) Other modularized solutions (*e.g.*, STN and ETN).

**Learning PT instead of affine.** As illustrated in Figure 2 and formulated in Equation 1, both affine transformation and PT for two-dimensional images are linear geometric transformations that can be represented by a  $3 \times 3$  matrix in homogeneous coordinates. However, because the degree of freedom [Andrew, 2001] is 8 for a PT and is 6 for an affine (For affine,  $\theta_{3,1}$  and  $\theta_{3,2}$  in Equation 2, *i.e.*, the projection vector, are always 0), the affine transformation is a special case of PT. As a result, the affine transformation has to preserve parallelism while the PT does not preserve parallelism, length, or

angle. This enables the PT to not only reflect the observer's viewpoint changes but also model the geometries in affine (*i.e.*, rotation, scaling, translation, and shearing).

**An adjustable number of TMs.** Instead of using a CNN block to learn a single TM in STN and ETN, the number of TMs is a tunable hyperparameter of the proposed PT layer. There are two main reasons. First, a single PT layer can learn different viewpoints to facilitate the analysis of the subsequent layers. For example, to better classify one object on an image, we may need to provide the views from both the left and right of the object. Second, in deep learning frameworks, being able to adjust the number of TMs enables an tunable learning capacity. For example, we can increase the filter numbers to enhance the learning capacity for a convolutional layer. Similarly, increasing the number of TMs will also increase the learning capacity for the proposed PT layer.

**A layer instead of a module.** Our proposed method introduces a layer instead of module which can be trained in a similar manner to a convolutional layer. Thus, a proposed PT layer directly applies gradient descent to train its TMs, which does not create any to-be-trained module parameters. In comparison, existing modularized solutions creates extra module parameters, *e.g.*, in STN, a typical TM learning module introduces 36,000 extra training parameters with two convolutional and two fully-connected layers, although one could customize the layers in the module.

Figure 3 presents the details of the proposed PT layer. The layer input is defined as  $I \in \mathbb{R}^{N \times H \times W \times C}$  where  $H$  denotes the height,  $W$  is the width,  $C$  represents the channels, and  $N$  is the batch size. A PT layer learns  $M$  TMs where  $M$  is tunable. Each TM  $\theta^m \in \mathbb{R}^{3 \times 3}$ ,  $m = 1, 2, \dots, M$  is applied to the PT of all the input channels. Hence, the layer output can be defined as  $O \in \mathbb{R}^{N \times H \times W \times (C \times M)}$  that has  $C \times M$  channels.

### 3.2 Transformation and Interpolation

This section discusses the mathematical details of the proposed PT layer. Defining  $i$ -th input feature map of the proposed PT layer as  $I_i \in \mathbb{R}^{H \times W \times C}$ , its input pixel of  $c$ -th channel ( $c \in [1, C]$ ) at location  $(x, y)$  as  $I_{x,y}^c$ , and its corresponding  $i$ -th output feature map as  $O_i \in \mathbb{R}^{H \times W \times C}$ , the PT on the homogeneous coordinates can be written as:

$$\begin{pmatrix} x' \\ y' \\ \omega \end{pmatrix} = \theta^m \begin{pmatrix} x \\ y \\ 1 \end{pmatrix}, \quad (1)$$

where  $\theta^m$  is the to-be-learned  $m$ -th TM

$$\theta^m = \begin{bmatrix} \theta_{1,1} & \theta_{1,2} & \theta_{1,3} \\ \theta_{2,1} & \theta_{2,2} & \theta_{2,3} \\ \theta_{3,1} & \theta_{3,2} & 1 \end{bmatrix}, \quad (2)$$

and  $(x', y', \omega)$  is the target coordinates of the output feature map, where  $\omega$  represents the distance between the camera and the image plane. For interpolation, we convert the homogeneous coordinates back to euclidean coordinates by

$$(x'', y'') = (x'/\omega, y'/\omega). \quad (3)$$

Having the original location  $(x, y)$  and the new target location  $(x'', y'')$ , we perform bilinear interpolation to produce the output feature map of PT, which can be formulated below:

$$O_i^c = \sum_x^H \sum_y^W I_{x,y}^c K(x'' - x, y'' - y), \quad (4)$$

where  $K(\cdot, \cdot)$  is a kernel function. For bilinear interpolation, the kernel function can be written as:

$$K(x, y) = K_1(u)K_1(v), \quad K_1(t) = |1 - \lfloor t \rfloor|, \quad (5)$$

and Equation 4 can be reduced to:

$$O_i^c = \sum_x^H \sum_y^W I_{x,y}^c |1 - \lfloor x'' - x \rfloor| \cdot |1 - \lfloor y'' - y \rfloor|. \quad (6)$$

By far, we have presented the the mathematical formulation of the transformation and interpolation inside the proposed PT layer.

### 3.3 Back-propagation

In this subsection, we show that the proposed PT layer is differentiable so that the TMs can be updated by gradient descent. To demonstrate the back-propagation, we show the derivative computation of the proposed PT layer where there are two major operations: the transformation and interpolation. First of all, it is apparent that the derivative of the coordinate transformation in Equation 1 is  $(x, y, 1)^T$ . Notably, each TM ( $\theta^m$ ) is applied in the PT of all input channels. Thus, each TM affects multiple coordinates  $(x, y)$ . To update the parameters in a TM  $\theta^m$ , we average all the derivatives obtained from all the affected coordinates.

For the bilinear interpolation in Equation 6, we show its gradients by computing the partial derivatives of  $i$ -th feature map output in channel  $c$  (*i.e.*,  $O_i^c$ ) with respect to  $I_{x,y}^c$ ,  $x''$ , and  $y''$ :

$$\frac{\partial O_i^c}{\partial I_{x,y}^c} = \sum_v^H \sum_t^W |1 - \lfloor x'' - x \rfloor| \cdot |1 - \lfloor y'' - y \rfloor|, \quad (7)$$

$$\frac{\partial O_i^c}{\partial x''} = \sum_v^H \sum_t^W I_{x,y}^c |1 - \lfloor y'' - y \rfloor| \cdot \alpha, \quad (8)$$

here  $\alpha$  is formulated as:

$$\alpha = \begin{cases} 1, & \lfloor x'' - x \rfloor > 1 \\ -1, & \lfloor x'' - x \rfloor < 0 \end{cases} \quad (9)$$

and similarly we can obtain  $\partial O_i^c / \partial y''$ .

Therefore, the proposed PT layer is differentiable so that (i) each of its TM can be trained by gradient descent; and (ii) the gradient can flow through this layer and it is stackable in deep neural networks in a similar manner with traditional layers such as a convolutional layer.

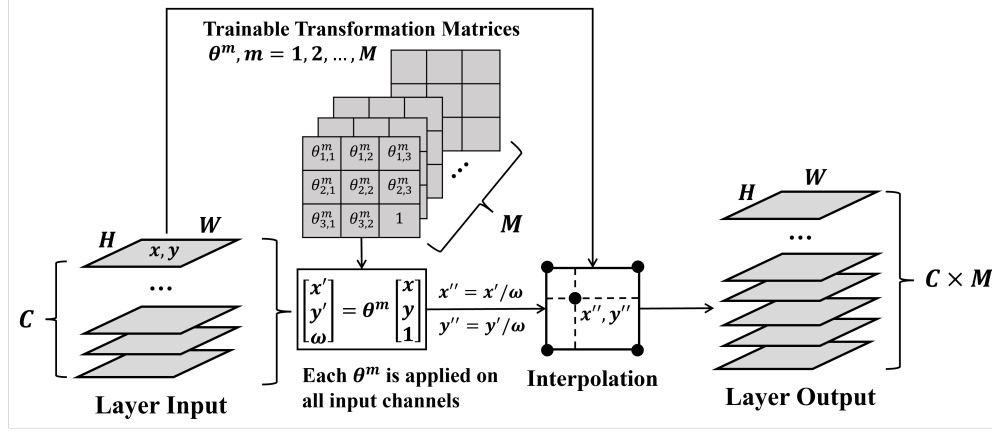


Figure 3: Details of the proposed PT layer.

## 4 Experiments and Analysis

This section experimentally analyzes quantitative and analytical evaluation of the proposed PT layer. Section 4.1 introduces our data preparation. Section 4.2 validates the functionality of the proposed PT layer by learning known target PTs. Section 4.3 discusses the ablation study that compares the performance with and without the PT layer. Finally, section 4.4 compares the performance of the proposed PT layer against other well-known modules for geometric transformations.

### 4.1 Data Preparation

**MNIST.** The modified national institute of standards and technology database (MNIST) [Lecun *et al.*, 1998] is a standard dataset of handwritten digits that consists of 60,000 training and 10,000 testing grayscale images of size  $28 \times 28$ . For our training dataset, we apply random PTs on 55,000 images and leave the remaining 5,000 unmodified. Some images are left unmodified since the unmodified images can provide the original geometric information to the PT layer. For the testing set, we apply random PTs on all 10,000 images. Figure 4 shows a few examples of randomly transformed MNIST images.



Figure 4: A few MNIST images with random PTs.

**SVHN.** The street view house numbers dataset (SVHN) [Netzer *et al.*, 2011] is a real-world dataset containing 73,257 training and 26,032 testing RGB color images of size  $32 \times 32$  (examples in Figure 5). The SVHN can facilitate our experiments because the street number images are collected by cameras that introduce various viewpoints. In our experiments, we show that the PT layers can learn good PTs (viewpoints) to help a downstream classifier that recognizes the street numbers.

**Imagenette.** The Imagenette [Howard, 2019] is a subset of 10 representative classes from the huge Imagenet dataset [Deng *et al.*, 2009]. The Imagenette dataset includes 9,469 training and 3,925 testing RGB images of various

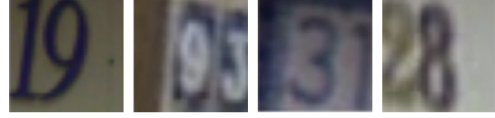


Figure 5: A few SVHN images.

sizes. Out of these, we use the ones with  $320 \times 320$  size and resized them to  $224 \times 224$ . We adopt this representative and small version of the Imagenet for two main reasons: (i) the Imagenette validates the proposed PT layer with larger ( $224 \times 224$ ) images compared to the MNIST and the SVHN; and (ii) rather than applying all the 1,000 classes with more than millions of images from the Imagenet, the Imagenette provides a fast reproducibility. In our experiments, for the training set of 9,469 images, we apply random PTs on approximately 8,285 images (87.5%) and leave the remaining 1,184 images (12.5%) unmodified. For the 3,925 testing images we use the same split of transformed and unmodified images. Figure 6 shows a few examples of randomly transformed Imagenette images.



Figure 6: A few Imagenette images with random PTs.

### 4.2 Functionality Validation

This section validates the fundamental functionality of the proposed PT layer. As a layer designed to learn different PTs or viewpoints, the proposed PT layer should be able to easily rectify the inputs transformed by PTs if the original images are given as the labels.

**Experiments scheme.** As illustrated in Figure 7, we create a simple model with two PT layers (each layer has only 1 TM) where the model inputs are the MNIST images with PTs, and the outputs are the undistorted images. We train this model by minimizing the mean squared error (MSE) between the model outputs and the original images.

**Results.** This simple two-layer model can easily learn the rectifications within a few epochs. Although we actually find that even a single PT layer can learn this rectification, we present this two-layer model to illustrate a progressive transformation of each PT layer towards the final target (see a few



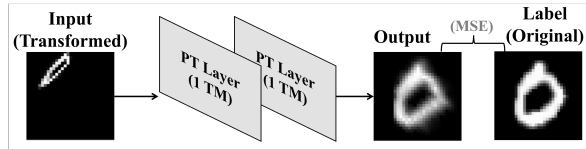


Figure 7: The process of the functionality validation.

examples in Figure 8). The results of the two-layer model not only demonstrate the functionality of the PT layers, but also show that the PT layers are stackable (the gradients flow through it) in a deep learning framework.

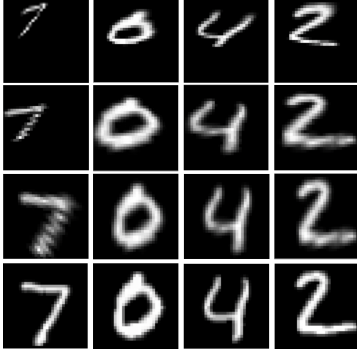


Figure 8: Examples from functionality validation with a two PT layer model. Top row: The input transformed MNIST images; Second row: Outputs of the first PT layer; Third row: Outputs of the second PT layer; Last row: The target original MNIST images.

### 4.3 Ablation Study

This section demonstrates the advantage of using the proposed PT layer. In addition to a common ablation study that compares the performance of a model with and without PT layer(s), we also test the effect of different inserting positions and multiple PT layers.

**Experiments scheme.** As presented in Figure 9, we adopt the G-CNN [Cohen and Welling, 2016] (all convolutional layers have 32 filters) and select the places after the input, the first, the second, and the third convolutional layers as the inserting positions of a PT layer. To empirically test a good position for the PT layer, we insert a PT layer (with four TMs) at one position at a time. And to test multiple PT layers in a model, we also test the case of placing a PT layer at all the positions mentioned above.

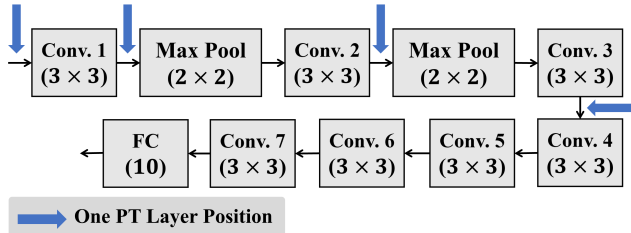


Figure 9: The model of our ablation study.

The ablation study is performed on the transformed MNIST and the SVHN. We train the models for 25 and 30 epochs respectively with the goal of classification using categorical cross-entropy as the loss function, which is minimized by the ADAM optimizer [Kingma and Ba, 2015] at a starting

learning rate of 0.0001. It is worth noting that we add a  $1 \times 1$  convolutional layer after the PT layer with number of filters equal to the number of channels of the input of PT layer to summarize the output channels, so that the channel shape of the feature maps becomes the same before and after the PT layer.

**Results.** Table 1 shows the classification testing accuracy, where one can observe that inserting the PT layer(s) improves the classification performance (the baseline model is the one without any PT layers). Furthermore, the empirically best positions of a PT layer are the positions after the first convolution or after the input. Finally, placing a PT layer at all the selected positions achieves the best accuracy, which indicates that increasing the number of PT layers can enhance the performance of a model. Notably, given a model, the number of PT layers and the inserting positions are tunable hyperparameters in deep learning frameworks.

Architecture (G-CNN)	Accuracy % (MNIST)	Accuracy % (SVHN)
Baseline	95.97	89.56
After input	96.55	90.06
After conv. 1	96.22	90.89
After conv. 2	96.37	90.38
After conv. 3	96.41	90.3
All positions	97.2	91.35

Table 1: Classification results with and without the PT layer at different positions.

In addition, we have validated that each trained TM in a PT layer is different, so that various possible viewpoint options are learned and offered to the successive layers. Figure 10 shows an example image and its learned viewpoints.

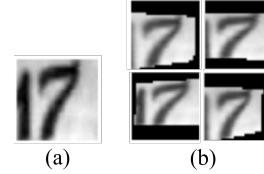


Figure 10: An example of learned viewpoints. (a) An input image; (b) Its various views learned by the PT layer.

### 4.4 Comparison Experiments

In this section, we compare the performance of the proposed PT layer against the STN and ETN modules on our datasets. Specifically, to extract geometric features, the proposed PT layer, the STN module, and the ETN module are respectively inserted after the input of a baseline model, and the classification accuracies are compared. For our PT layer, we also experiment with increasing the number of TMs  $M$ . It is worth noting that constructing an ETN module requires providing information about the order and type of distortion to its transformer layers. In contrast, the proposed PT layer and the STN do not need any prior knowledge of the distortions. In this comparison experiment, we provide the following prior knowledge to the ETN: the distortion consists of a translation, a PT on the horizontal axis, a PT on the vertical axis, and a scaling on the horizontal axis.



Figure 11: Visualizations of the layer or module outputs. Top row: Input images; Second row: outputs of the STN; Third row: outputs of the ETN; Last row: outputs of PT layer.

**Experiments scheme.** We use the well-known CNN architecture ResNet18 [He *et al.*, 2016] that has 18 layer and residual connections as the baseline model for our SVHN and transformed MNIST. For the sake of faster training on the transformed Imagenette, we fine-tune the famous CNN architecture VGG16 [Simonyan and Zisserman, 2015] that was pretrained on the Imagenet dataset. The models are trained with the goal of classification using categorical cross-entropy as the loss, which is minimized by the ADAM optimizer at a starting learning rate of 0.0001.

Architecture	Accuracy % (MNIST) (ResNet-18)	Accuracy % (SVHN) (ResNet-18)	Accuracy % (Imagenette) (VGG-16)
Baseline	97.63	92.23	81.4
STN	97.74	92.56	82.96
ETN	97.68	92.42	86.6
PTL-4	97.66	92.49	87.62
PTL-8	97.74	92.84	90.42
PTL-16	97.87	93.16	91.31
PTL-32	97.95	93.44	91.26

Note: PTL- $x$  denotes a PT layer with  $x$  TMs ( $x = 4, 8, 16, 32$  here).

Table 2: Comparison of PT layer with the STN and ETN on the transformed MNIST, SVHN and Imagenette.

**Results.** Table 2 demonstrates that the proposed PT layer has better classification accuracies compared to both the baseline model and the models with ETN and STN modules. The PT layer has a significant impact on more complicated datasets such as the Imagenette, where we observe an approximately 10% increase in accuracy. Furthermore, increasing the number of TMs has a positive impact on increasing the classification accuracy. This is due to the enhanced learning capacity of PT layers with more TMs. The number of TMs is a tunable hyperparameter for the proposed PT layer.

To provide a visual comparison, we visualize some after-layer and after-module outputs from the PTL-4, the STN, and the ETN. Some example input images and their corresponding outputs of the PT layer and the STN and ETN modules are shown in Figure 11. Compared to the STN and the ETN, the proposed PT layer learns good viewpoints (we are just displaying one of them) without cropping out the objects, high-

lights (centralizes) the target objects, and has smaller changes to the overall pixel intensities.

**Discussion of attention and weak supervision applications.** Analogous to the state-of-the-art methods, the proposed PT layer has potentials in applications of spatial attention [Jaderberg *et al.*, 2015] and weak supervision [Pan *et al.*, 2019]. Figure 12 shows one of many examples in the datasets. We explain these potentials using a PTL-1’s outputs of an example input image with two digits. When recognizing each digit on this two-digit image, the PT layer can learn to concentrate on the correct target digit with a viewpoint. This concentration outcome can facilitate spatial attention where we need to learn the highlight of certain parts on images to help downstream tasks. Furthermore, the PT layer has the potential to assist weak supervision with inexact labels: when only providing classification labels to a deep learning model, the PT layer could also learn to centralize and localize the to-be-classified object, and thus learning the object location on the images with only classification labels.

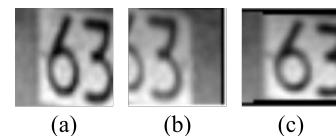


Figure 12: An example visual attention. (a) The input image containing two digits; (b) and (c) The outputs of a PTL-1 when classifying it as "3" and "6" respectively.

## 5 Conclusion

This paper introduces a PT layer that extracts geometric features for images in deep learning. The proposed PT layer models viewpoints which is more general than affine transformations, provides the learning of multiple PTs which results in an adjustable learning advantage, and facilitates its training with directly differentiable operations on the TMs. Experimentally, we have validated the basic functionality of the proposed PT layer, confirmed the PT layer’s promising performance by the ablation study, and demonstrated our superiority as compared to other state-of-the-art methods. At the next step, we will explore more practicality of the proposed PT layer, especially in 3-dimensional views.

## References

- [Andrew, 2001] Alex M Andrew. Multiple view geometry in computer vision. *Kybernetes*, 30:1333–1341, 2001.
- [Cohen and Welling, 2016] Taco Cohen and Max Welling. Group equivariant convolutional networks. In *Proc. ICML*, volume 48, pages 2990–2999, New York, New York, USA, 20–22 Jun 2016. PMLR.
- [Deng *et al.*, 2009] Jia Deng, Wei Dong, Richard Socher, Li Jia Li, Kai Li, and Li Fei-Fei. Imagenet: A large-scale hierarchical image database. In *Proc. CVPR*, pages 248–255, 2009.
- [Detlefsen *et al.*, 2018] Nicki Skaftø Detlefsen, Oren Freifeld, and Søren Hauberg. Deep diffeomorphic transformer networks. In *Proc. CVPR*, June 2018.
- [Esteves *et al.*, 2018] Carlos Esteves, Christine Allen-Blanchette, Xiaowei Zhou, and Kostas Daniilidis. Polar transformer networks. In *ICLR*, 2018.
- [Garau *et al.*, 2021] Nicola Garau, Niccolò Bisagno, Piotr Bródka, and Nicola Conci. DECA: Deep viewpoint-Equivariant human pose estimation using Capsule Autoencoders. In *Proc. CVPR*, pages 11677–11686, 2021.
- [He *et al.*, 2016] Kaiming He, Xiangyu Zhang, Shaoqing Ren, and Jian Sun. Deep residual learning for image recognition. In *Proc. CVPR*, pages 770–778, 2016.
- [Howard, 2019] Jeremy Howard. Imagenette. <https://github.com/fastai/imagenette/>, 2019. [Online; accessed January 2022].
- [Huang *et al.*, 2017] Gao Huang, Zhuang Liu, Laurens Van Der Maaten, and Kilian Q Weinberger. Densely connected convolutional networks. In *Proc. CVPR*, pages 4700–4708, 2017.
- [Jaderberg *et al.*, 2015] Max Jaderberg, Karen Simonyan, Andrew Zisserman, and Koray Kavukcuoglu. Spatial transformer networks. *NeurIPS*, 28:2017–2025, 2015.
- [Kingma and Ba, 2015] Diederik P. Kingma and Jimmy Ba. Adam: A method for stochastic optimization. In *ICLR (Poster)*, 2015.
- [Krasheninnikov and Potapov, 2012] V.R. Krasheninnikov and M.A. Potapov. Estimation of parameters of geometric transformation of images by fixed-point method. *Pattern Recognit. Image Anal.*, 22(2):303–317, 2012.
- [Lecun *et al.*, 1998] Y. Lecun, L. Bottou, Y. Bengio, and P. Haffner. Gradient-based learning applied to document recognition. *Proc. IEEE*, 86(11):2278–2324, 1998.
- [Lin and Lucey, 2017] C. Lin and S. Lucey. Inverse compositional spatial transformer networks. In *CVPR*, pages 2252–2260, Los Alamitos, CA, USA, July 2017. IEEE Computer Society.
- [Lowe, 2004] David G Lowe. Distinctive image features from scale-invariant keypoints. *Int. J. Comput. Vis.*, 60(2):91–110, 2004.
- [Lucas and Kanade, 1981] Bruce D. Lucas and Takeo Kanade. An iterative image registration technique with an application to stereo vision. In *Proc. IJCAI*, IJCAI’81, page 674–679, San Francisco, CA, USA, 1981. Morgan Kaufmann Publishers Inc.
- [Netzer *et al.*, 2011] Yuval Netzer, Tao Wang, Adam Coates, Alessandro Bissacco, Bo Wu, and Andrew Y Ng. Reading digits in natural images with unsupervised feature learning. In *NeurIPS*, 2011.
- [Pan *et al.*, 2019] Tianxiang Pan, Bin Wang, Guiguang Ding, Jungong Han, and Junhai Yong. Low shot box correction for weakly supervised object detection. In *Proc. IJCAI*, pages 890–896. International Joint Conferences on Artificial Intelligence Organization, 7 2019.
- [Papernot *et al.*, 2016] Nicolas Papernot, Patrick McDaniel, Somesh Jha, Matt Fredrikson, Z Berkay Celik, and Ananthram Swami. The limitations of deep learning in adversarial settings. In *IEEE EuroS&P*, pages 372–387. IEEE, 2016.
- [Sabour *et al.*, 2017] Sara Sabour, Nicholas Frosst, and Geoffrey E Hinton. Dynamic routing between capsules. In *NeurIPS*, volume 30. Curran Associates, Inc., 2017.
- [Simonyan and Zisserman, 2015] Karen Simonyan and Andrew Zisserman. Very deep convolutional networks for large-scale image recognition. In *ICLR*, 2015.
- [Tai *et al.*, 2019] Kai Sheng Tai, Peter Bailis, and Gregory Valiant. Equivariant transformer networks. In *ICLR*, pages 6086–6095. PMLR, 2019.
- [Wang *et al.*, 2018] Fangfang Wang, Liming Zhao, Xi Li, Xinchao Wang, and Dacheng Tao. Geometry-aware scene text detection with instance transformation network. In *Proc. CVPR*, pages 1381–1389, 2018.
- [Wang *et al.*, 2019] Ning Wang, Jingyuan Li, Lefei Zhang, and Bo Du. Musical: Multi-scale image contextual attention learning for inpainting. In *Proc. IJCAI*, pages 3748–3754. International Joint Conferences on Artificial Intelligence Organization, 7 2019.
- [Xu *et al.*, 2018] Huapeng Xu, Guilin Qi, Jingjing Li, Meng Wang, Kang Xu, and Huan Gao. Fine-grained image classification by visual-semantic embedding. In *Proc. IJCAI*, pages 1043–1049. International Joint Conferences on Artificial Intelligence Organization, 7 2018.
- [Yan *et al.*, 2016] Xinchun Yan, Jimei Yang, Ersin Yumer, Yijie Guo, and Honglak Lee. Perspective transformer nets: Learning single-view 3d object reconstruction without 3d supervision. In *NeurIPS, NIPS’16*, Red Hook, NY, USA, 2016. Curran Associates Inc.
- [Zhou *et al.*, 2017] Yiren Zhou, Sibong Song, and Ngai-Man Cheung. On classification of distorted images with deep convolutional neural networks. In *Proc. ICASSP IEEE Int. Conf. Acoust. Speech Signal Process*, pages 1213–1217. IEEE, 03 2017.